Noise-induced bistability in a simple mutual inhibition system

Taichi Haruna [*]
Department of Information and Sciences, School of Arts and Sciences, Tokyo Woman's Christian University, 2-6-1 Zempukuji, Suginami-ku, Tokyo 167-8585, Japan

Tomohiro Shirakawa [†]
Department of Information and Management Systems Engineering, Graduate School of Engineering, Nagaoka University of Technology, 1603-1 Kamitomioka, Nagaoka, Niigata 940-2188, Japan

(Received 21 November 2022; accepted 14 July 2023; published 7 August 2023)

In this study, we study noise-induced bistability in a simple bivariate mutual inhibition system with slow fluctuating responses to external signals. We give a general condition that the marginal stationary probability density of one of the two variables experiences a transition from a unimodal shape to a bimodal one. We show that the transition occurs even when the stationary probability density of the response to external signals is monotone. The mechanism for the transition is investigated in terms of the calculation of the mean first passage time. We also discuss the genericity of the transition mechanism.

DOI: 10.1103/PhysRevE.108.024108

I. INTRODUCTION

Noise can induce nontrivial phenomena in nonlinear systems, including noise-induced order in one-dimensional iterated maps [1], noise-induced stability in high-dimensional recurrent neural networks [2], noise-induced synchronization in phase oscillators [3], noise-induced oscillations in population dynamics [4] and gene regulatory cirtuits [5], and noise-induced bistability in autocatalytic systems [6–8] and mutual inhibition systems [9]. Such noise-induced phenomena sometimes play functional roles in biological systems [10–12]. In this paper, we present noise-induced bistability with a mechanism inspired by a recent experiment on the true slime mold [13].

Shirakawa *et al.* studied the behavior of the plasmodium of the true slime mold *Physarum polycephalum* when it was presented with a contradictory situation [13]. In this experiment, they gave the plasmodium stimuli consisting of a mixture of an attractant and a repellant. The responses of the plasmodium to the stimuli were diverse: the degree of attraction or repulsion varied trial by trial, even though the concentrations of attractant and repelllant were fixed and the samples used were clones split from the same cell. To explain the diverse responses of the plasmodium, Shirakawa *et al.* constructed a simple signal transduction network model that replicated the experimental results, at least qualitatively. The molecular species comprised in the model were signal transducers x_a and x_r for the attractant and repellant signals, receptors y_a and y_r for the attractant and the repellant, and an activating factor z for cell motility. The signal transduction network model assumes that y_a and y_r are not only taken as the receptors but also the attractant and repellant stimuli, the signal transducers x_a and x_r mutually inhibit each other, and the cell motility z is activated by x_a but inhibited by x_r. The model equations were given by

$$\frac{dx_a}{dt} = v_{x_a}\frac{y_a^2}{K_{y_a}+y_a^2}\frac{K_{x_r,1}}{K_{x_r,1}+x_r} - d_{x_a}x_a, \quad (1)$$

$$\frac{dx_r}{dt} = v_{x_r}\frac{y_r^2}{K_{y_r}+y_r^2}\frac{K_{x_a,1}}{K_{x_a,1}+x_a} - d_{x_r}x_r, \quad (2)$$

$$\frac{dz}{dt} = v_z\frac{x_a}{K_{x_a,2}+x_a}\frac{K_{x_r,2}}{K_{x_r,2}+x_r} - d_z z, \quad (3)$$

where v_{x_a}, v_{x_r}, and v_z are the reaction rates, K_{y_a}, K_{y_r}, $K_{x_a,1}$, $K_{x_r,1}$, $K_{x_a,2}$, and $K_{x_r,2}$ are the dissociation constants, and d_{x_a}, d_{x_r}, and d_z are the degradation rates.

Shirakawa *et al.* numerically simulated Eqs. (1)–(3) with y_a and y_r sampled from given normal distributions at each time step. For certain model parameter values, they found that the stationary probability density of z shows "weak bimodality": the density has a main single peak with a bump at its tail. Note that it is straightforward to see that Eqs. (1) and (2) have a single globally stable solution (x_a^*, x_r^*) when y_a and y_r are fixed. Then, the stationary value of z is obtained by substituting (x_a^*, x_r^*) into the right-hand side of Eq. (3). Thus the numerically observed weak bimodality is expected to originate from the interplay between the fluctuations of y_a and y_r and the nonlinearity of the model equations.

In what follows, we investigate the mechanism behind weak bimodality using stochastic differential equations [14]. We extract the core of the model equations proposed by Shirakawa *et al.*, which seem to be essential for weak bimodality, and reformulate them as stochastic differential equations. We show that our model does not exhibit weak bimodality but genuine bimodality instead. We give general conditions for the emergence of bimodality. Thus the aim of this paper is not

[*]tharuna@lab.twcu.ac.jp
[†]shirakawa@vos.nagaokaut.ac.jp

to directly explain weak bimodality observed by Shirakawa *et al.*, but to reveal the mechanism of noise-induced bistability hidden in their model. However, in the Supplemental Material [15], we study the model equations including all of x_a, x_r, and z, and discuss the origin of weak bimodality.

The remainder of this paper is organized as follows. In Sec. II, we describe our model equations. In Sec. III, we derive a general necessary and sufficient condition for the transition from a unimodal density to a bimodal density and examine its mechanism in terms of the calculation of the mean first passage time. Finally, in Sec. IV, we discuss the genericity of the noise-induced transition and its difference from known mechanisms of noise-induced bistability.

II. MODEL

Our model consists of the following differential and stochastic differential equations:

$$\frac{dx_a}{d\tau} = \frac{u_a}{x_r+1} - x_a, \tag{4}$$

$$\frac{dx_r}{d\tau} = \frac{u_r}{x_a+1} - x_r \tag{5}$$

and

$$du_a = A_a(u_a)dt + \sqrt{B_a(u_a)}dW_a, \tag{6}$$

$$du_r = A_r(u_r)dt + \sqrt{B_r(u_r)}dW_r, \tag{7}$$

where x_a and x_r are signal transducers for the attractant and repellant signals, u_a and u_r represent the activity of the receptors in response to the attractant and the repellant (see the next paragraph), W_a and W_r are independent Wiener processes, and $\tau = \alpha t$ with $\alpha \gg 1$. $\alpha \gg 1$ implies a difference in the time scales between (x_a, x_r) and (u_a, u_r), namely, the change of (u_a, u_r) is much slower than that of (x_a, x_r). We restrict the ranges of u_a and u_r to the intervals $[0, \nu_a]$ and $[0, \nu_r]$, respectively, and we impose the reflecting boundary conditions on Eqs. (6) and (7). At present, we do not specify the forms of the drift terms $A_a(u_a)$ and $A_r(u_r)$ or the diffusion terms $B_a(u_a) \geqslant 0$ and $B_r(u_r) \geqslant 0$ in Eqs. (6) and (7). Although all of the dissociation constants and degradation rates are taken to be 1 in Eqs. (4) and (5), we do not lose generality so long as $\alpha \gg 1$ holds, which implies Eq. (8) in Sec. III A below. We write X_a, X_r, U_a, and U_r for the stochastic variables corresponding to x_a, x_r, u_a, and u_r, respectively.

For simplicity, we assume that the cell motility z is identical to x_a and study the transition from a unimodal stationary probability density to a bimodal one for x_a. Indeed, we consider the model equations including z in addition to x_a and x_r in the Supplemental Material [15]. We show that the same kind of transition occurs for z, although the transition condition for z has a more complicated form than that for x_a given in Sec. III A below [Eq. (18)]. In the Supplemental Material [15], we also investigate the origin of weak bimodality found in the original model of Shirakawa *et al.* [13]. We show that weak bimodality can be recovered when the time-scale separation introduced above is weakened. Indeed, it is not unreasonable to think that the time-scale separation does not hold for the numerical results in Shirakawa *et al.* [13]. In the original model, the fluctuations of y_a and y_r are imposed at every time step of numerical simulations of Eqs. (1)–(3), although they are not modeled as stochastic differential equations.

To fit the setting of Eqs. (1)–(3) into the above general framework, one first could model the dynamics of the attractant y_a and the repellant y_r using Ornstein-Uhlenbeck processes whose stationary probability densities are Gaussian distributions. One would then consider the change of variables $u_a = \nu_a \frac{y_a^2}{1+y_a^2}$ and $u_r = \nu_r \frac{y_r^2}{1+y_r^2}$, where the dissociation constants are assumed to be 1 without loss of generality. Finally, one derives the stochastic differential equations governing the time evolution of u_a and u_r by applying Ito's formula. However, we do not study this example but consider an analytically solvable one in Sec. III for clarity and simplicity.

III. RESULTS

In this section, we derive the general condition that the stationary probability density of X_a has a peak at $x_a = 0$. If it has another peak in $x_a > 0$, we obtain a bimodal probability density. We give an analytically solvable example in which the transition from a single peak density to a bimodal density actually happens. We also calculate the mean first passage time of X_a from $x_a = 0$ to a given positive value of x_a. This will shed a different light on the mechanism behind the transition.

A. Stationary probability density

Under the assumption of the time-scale separation between (x_a, x_r) and (u_a, u_r), we expect that the solutions of Eqs. (4)–(7) satisfy

$$\frac{dx_a}{d\tau} = \frac{dx_r}{d\tau} = 0. \tag{8}$$

Let $P(x_a, x_r)$ be the stationary joint probability density of (X_a, X_r), Q_a the stationary probability density of U_a, and Q_r the stationary probability density of U_r. Equation (8) defines the change of variables

$$u_a = x_a(x_r + 1), \tag{9}$$

$$u_r = x_r(x_a + 1). \tag{10}$$

Geometrically, this change of variables can be described as follows. Let (x_a^*, x_r^*) be the positive solution of Eq. (8) with $u_a = \nu_a$ and $u_r = \nu_r$. Explicitly, $x_a^* = \frac{\nu_a - \nu_r - 1 + \sqrt{(\nu_a-\nu_r-1)^2 + 4\nu_a}}{2}$ and $x_r^* = x_a^* - \nu_a + \nu_r$. The change of variables Eqs. (9) and (10) defines a one-to-one correspondence between the rectangle $[0, \nu_a] \times [0, \nu_r]$ in the u_a-u_r plane and the region in the x_a-x_r plane enclosed by the x_a axis, x_r axis, $x_r = \frac{\nu_r}{x_a+1}$, and $x_r = \frac{\nu_a}{x_a} - 1$. Note that the upper-right corner (ν_a, ν_r) of the rectangle $[0, \nu_a] \times [0, \nu_r]$ is mapped to (x_a^*, x_r^*), which is the intersection of $x_r = \frac{\nu_r}{x_a+1}$ and $x_r = \frac{\nu_a}{x_a} - 1$. We also note that $u_a = x_a$ on the x_a axis and $u_r = x_r$ on the x_r axis.

Using the change of variables Eqs. (9) and (10), we have

$$\begin{aligned} P(x_a, x_r) &= Q_a(u_a)Q_r(u_r)J(u_a, u_r|x_a, x_r) && (11)\\ &= Q_a[x_a(x_r+1)]Q_r[x_r(x_a+1)](x_a + x_r + 1), && (12) \end{aligned}$$

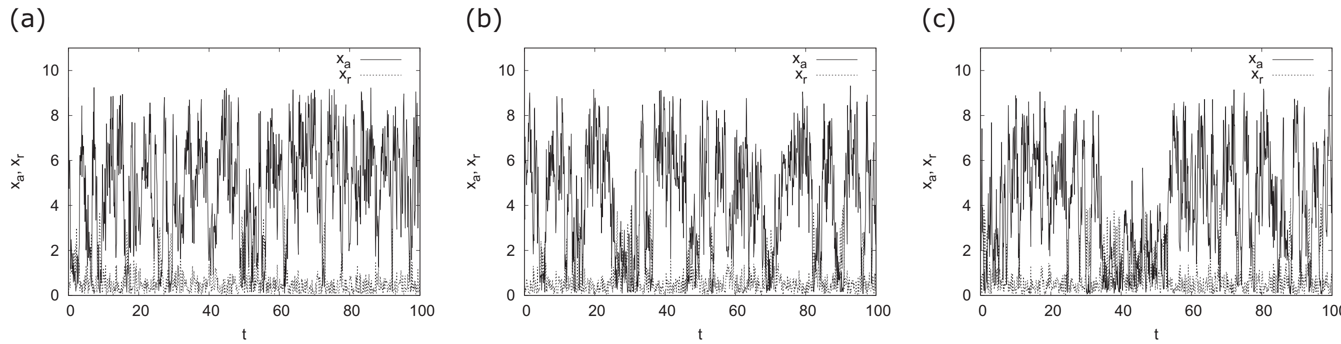

FIG. 1. Typical time series of x_a and x_r for the main example. (a) $\varepsilon = 1$. (b) $\varepsilon = 2.87$. (c) $\varepsilon = 5$. Those after ignoring the initial 10^4 transient steps are shown.

where $J(u_a, u_r|x_a, x_r)$ is the Jacobian matrix determinant of the change of variables from (x_a, x_r) to (u_a, u_r). $Q_a(u_a)$ and $Q_r(u_r)$ are explicitly given by [14]

$$Q_a(u_a) \propto \frac{1}{B_a(u_a)} \exp\left(2\int_0^{u_a} du_a' \frac{A_a(u_a')}{B_a(u_a')}\right), \tag{13}$$

$$Q_r(u_r) \propto \frac{1}{B_r(u_r)} \exp\left(2\int_0^{u_r} du_r' \frac{A_r(u_r')}{B_r(u_r')}\right). \tag{14}$$

The stationary probability density of X_a is obtained by marginalizing out X_r:

$$P_a(x_a) = \int_0^{\min\{\frac{\nu_r}{x_a+1}, \frac{\nu_a}{x_a}-1\}} dx_r P(x_a, x_r). \tag{15}$$

Similarly, the stationary probability density of X_r is

$$P_r(x_r) = \int_0^{\min\{\frac{\nu_a}{x_r+1}, \frac{\nu_r}{x_r}-1\}} dx_a P(x_a, x_r). \tag{16}$$

The condition that $P_a(x_a)$ has a peak at $x_a = 0$ is given by

$$\frac{dP_a}{dx_a}(0) < 0. \tag{17}$$

This is equivalent to (Appendix A)

$$\frac{d\ \ln Q_a}{du_a}(0) < \frac{2\langle U_r\rangle}{\langle (U_r+1)^2\rangle}, \tag{18}$$

where $\langle f(U_r)\rangle = \int_0^{\nu_r} du_r f(u_r) Q_r(u_r)$ is the expected value of $f(U_r)$ for a given function $f(u_r)$. Equation (18) means that $P_a(x_a)$ has a peak at 0 even if $\frac{dQ_a}{du_a}(0) > 0$ as long as U_r has a positive average and $\frac{dQ_a}{du_a}(0)$ is sufficiently small. Note that the left-hand side of Eq. (18) can be written explicitly in terms of A_a and B_a: since $Q_a(u_a) \propto e^{-\phi_a(u_a)}$ with a potential function $\phi_a(u_a) = -\int_0^{u_a} du_a' \frac{2A_a(u_a') - \frac{dB_a}{du_a}(u_a')}{B_a(u_a')}$, we have $\frac{d\ \ln Q_a}{du_a}(0) = -\frac{d\phi_a}{du_a}(0) = \frac{2A_a(0) - \frac{dB_a}{du_a}(0)}{B_a(0)}$.

Let us consider the case $A_a(u_a) = \frac{\Delta_a}{2(u_a+\varepsilon)}$, $B_a(u_a) = \Delta_a$, $A_r(u_r) = 0$, and $B_r(u_r) = \Delta_r$, where $\varepsilon \geqslant 0$ and $\Delta_a, \Delta_r > 0$. ε controls the strength of the drive toward greater activity by u_a. The larger ε is, the weaker the drive is. In what follows, we refer to this case as the main example. From Eqs. (13) and (14) and the normalization condition for the probability densities, we obtain

$$Q_a(u_a) = c_a(u_a + \varepsilon), \tag{19}$$

$$Q_r(u_r) = c_r, \tag{20}$$

where $c_a = \frac{1}{\frac{1}{2}\nu_a^2 + \nu_a\varepsilon}$ and $c_r = \frac{1}{\nu_r}$. Note that $Q_a(u_a)$ is a monotonically increasing function of u_a and approaches a constant function as ε increases. From Eq. (12), $P(x_a, x_r)$ is explicitly obtained as

$$P(x_a, x_r) = c_a c_r [x_a(x_r + 1) + \varepsilon](x_a + x_r + 1). \tag{21}$$

Using Eqs. (15) and (16), explicit expressions for $P_a(x_a)$ and $P_r(x_r)$ can also be obtained (Appendix B). By $\frac{d\ \ln Q_a}{du_a}(0) = \frac{2A_a(0) - \frac{dB_a}{du_a}(0)}{B_a(0)} = \frac{1}{\varepsilon}$ and an elementary calculation, Eq. (18) is reduced to

$$\varepsilon > \frac{\nu_r^2 + 3\nu_r + 3}{3\nu_r}, \tag{22}$$

which is a necessary and sufficient condition for $P_a(x_a)$ to have a peak at $x_a = 0$ in the case of Eq. (21).

Figures 1–3 show typical time series of x_a and x_r, $P_a(x_a)$ and $P_r(x_r)$ when $\varepsilon = 1$, 2.87, and 5, respectively. Here, we take $\Delta_a = 25$, $\Delta_r = 100$, $\nu_a = 10$, $\nu_r = 5$, and $\alpha = 100$. Equations (4)–(7) are numerically simulated using the Euler-Maruyama method with a time step $\delta t = 10^{-4}$. In this case, Eq. (22) becomes $\varepsilon > \varepsilon_{\text{crit}} = \frac{43}{15} \approx 2.87$. We can see that $P_a(x_a)$ has a single peak at $x_a = x_a^* = 2 + \sqrt{14} \approx 5.74$ when $\varepsilon = 1$, while it has another peak at $x_a = 0$ when $\varepsilon = 2.87$ and 5 (Fig. 2). When $\varepsilon = 2.87$ and 5, we observe that x_a switches from larger values to smaller values and vice versa in Figs. 1(b) and 1(c), which reflects the bimodal stationary densities in Figs. 2(b) and 2(c). In contrast to $P_a(x_a)$, $P_r(x_r)$ does not exhibit any qualitative change as ε increases (Fig. 3). We note that $P_a(x_a)$ begins to have the second peak at $x_a > 0$ when $\varepsilon = \frac{4\times 3^{\frac{1}{4}}\nu_r^{\frac{1}{2}} - 2\nu_r}{3} + 1 \approx 1.59$, which can be checked using elementary differential calculus. As ε is increased to $\varepsilon_{\text{crit}} \approx 2.87$, the position of the second peak approaches and reaches $x_a = 0$. Thus $P_a(x_a)$ is already a bimodal density even at $\varepsilon = 2.87$ as in Fig. 2(b). We also note that the peak at $x_a = x_a^*$ vanishes at $\varepsilon = 1 + \frac{3(x_a^*+1)^4 - 2\nu_r^2(x_a^*+1) + 3\nu_r^2}{3\nu_r(x_a^*+1)} = \frac{379}{15} + \frac{46\sqrt{14}}{5} \approx 59.69$, which can also be checked using elementary differential calculus.

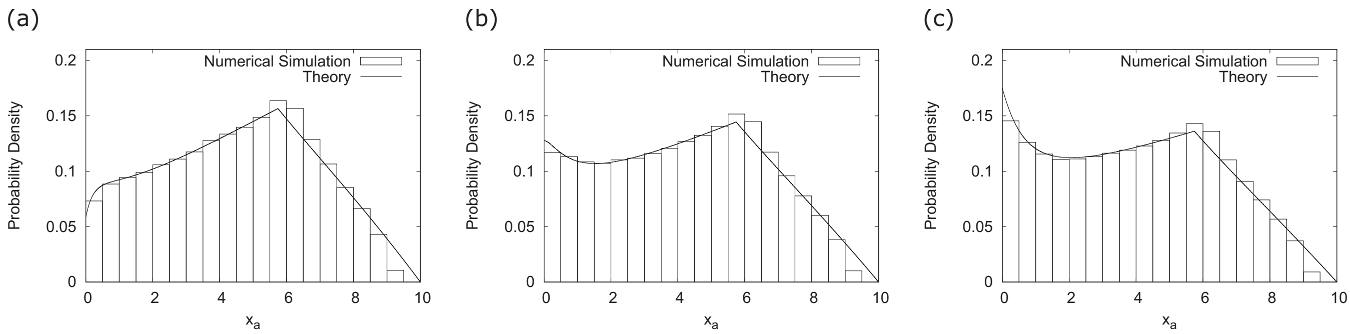

FIG. 2. Stationary probability density of x_a for the main example. (a) $\varepsilon = 1$. (b) $\varepsilon = 2.87$. (c) $\varepsilon = 5$. Numerical densities are obtained from a single trial of length 10^8 steps after ignoring the initial 10^4 transient steps.

The peak at $x_a = 0$ in $P_a(x_a)$ does not need any peak on the boundary $x_a = 0$ in $P(x_a, x_r)$. Since $P(x_a, x_r)$ is increasing in x_r on $x_a = 0$ as can be seen from Eq. (21), it must exist at $(x_a, x_r) = (0, \nu_r)$ if it actually exists. In general, the condition that $P(x_a, x_r)$ has a peak at $(x_a, x_r) = (0, \nu_r)$ is expressed as

$$\frac{\frac{\partial P}{\partial x_r}(0, \nu_r)}{\frac{\partial P}{\partial x_a}(0, \nu_r)} > -\alpha, \tag{23}$$

where α is the slope of the tangent line of $x_r = \frac{\nu_r}{x_a+1}$ at $(x_a, x_r) = (0, \nu_r)$. In the case of Eq. (21), Eq. (23) is reduced to

$$(\nu_r - 1)\varepsilon > (\nu_r + 1)^2, \tag{24}$$

which is $\varepsilon > 9$ when $\nu_r = 5$. Thus, when $2.87 \approx \varepsilon_{\text{crit}} < \varepsilon \leqslant 9$, $P_a(x_a)$ in the main example has a peak at $x_a = 0$, while $P(x_a, x_r)$ does not.

We note that $P(x_a, x_r)$ is a stationary solution of the stochastic differential equation governing the dynamics of (x_a, x_r), which can be obtained from Eqs. (6) and (7) together with the change of variables Eqs. (9) and (10) by using Ito's formula [14]. In Appendix C, we derive the stochastic differential equation for the above example and discuss how its drift and diffusion terms change when ε is varied.

B. Mean first passage time

We compute the mean first passage time $T_{X_a}(0, c)$ of X_a from 0 to c with $0 < c \leqslant x_a^*$. By using the change of variables Eqs. (9) and (10), this can be done as follows.

Let $0 < c \leqslant x_a^*$. First, observe that the lines $x_a = 0$ and $x_a = c$ in the x_a-x_r plane correspond to the lines $u_a = 0$ and $u_a = c(\frac{u_r}{c+1} + 1)$ in the u_a-u_r plane, respectively. Thus the desired first passage time can be computed in terms of the u_a-u_r plane. Assume that the initial probability density is stationary. Since the stochastic differential equations (6) and (7) for U_a and U_r are not coupled, we have

$$\begin{aligned} T_{X_a}(0, c) &= \int_0^{\nu_r} du_r Q_r(u_r) T_{U_a}\left[0, c\left(\frac{u_r}{c+1} + 1\right)\right] \\ &= \frac{c+1}{c} \int_c^{c(\frac{\nu_r}{c+1}+1)} du_a Q_r\left[(c+1)\left(\frac{u_a}{c} - 1\right)\right] \\ &\quad \times T_{U_a}(0, u_a), \end{aligned} \tag{25}$$

where $T_{U_a}(0, u_a)$ is the first passage time of U_a from 0 to u_a. $T_{U_a}(0, u_a)$ is obtained as [14]

$$T_{U_a}(0, u_a) = 2 \int_0^{u_a} \frac{du}{\psi(u)} \int_0^u dv \frac{\psi(v)}{B_a(v)}, \tag{26}$$

where $\psi(u) = \exp(\int_0^u dv \frac{2A_a(v)}{B_a(v)})$.

An explicit formula for $T_{X_a}(0, c)$ in the case $A_a(u_a) = \frac{\Delta_a}{2(u_a+\varepsilon)}$, $B_a(u_a) = \Delta_a$, $A_r(u_r) = 0$, and $B_r(u_r) = \Delta_r$ with $\varepsilon \geqslant 0$ and $\Delta_a, \Delta_r > 0$ is given in Appendix D.

In Fig. 4, we compare the theoretical predictions of the mean first passage time Eq. (D2) for $\varepsilon = 1,\ 2.87$, and 5 with numerical simulations. One can see that they agree well. The mean first passage time becomes larger as ε is increased. This is consistent with the fact that a peak emerges at $x_a = 0$

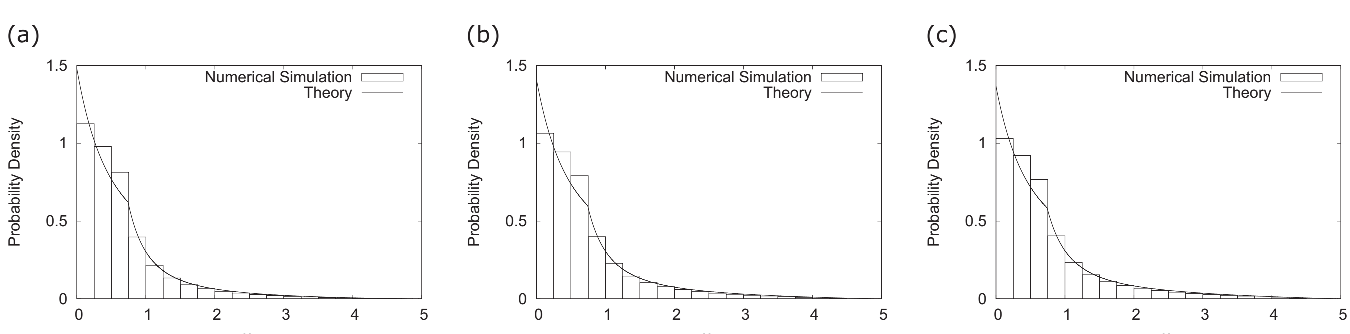

FIG. 3. Stationary probability density of x_r for the main example. (a) $\varepsilon = 1$. (b) $\varepsilon = 2.87$. (c) $\varepsilon = 5$. Numerical densities are obtained from a single trial of length 10^8 steps after ignoring the initial 10^4 transient steps.

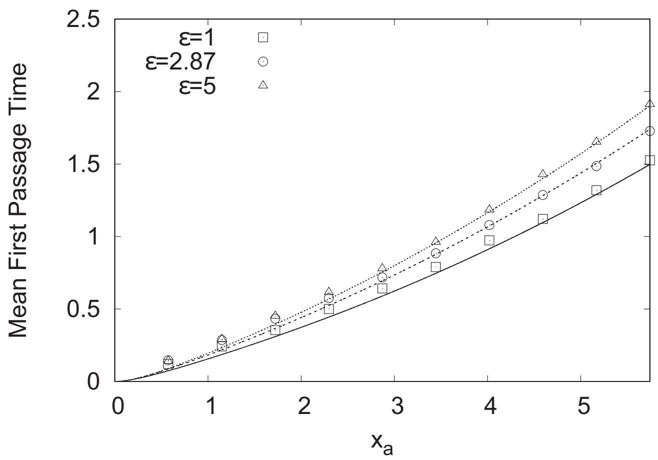

FIG. 4. Mean first passage time of x_a from 0 to $0 < c \leqslant x_a^*$ for the main example. Given a pair of values (ε, c), the average over 10^3 trials is taken. The initial condition for the numerical simulation is given as follows: $u_a(0) = 0$ and $u_r(0)$ is sampled from the stationary density of U_r, namely, the uniform distribution on $[0, \nu_r]$. $x_a(0)$ and $x_r(0)$ are then given by the formulas for the change of variables Eqs. (9) and (10). Marks are numerical simulations and lines are theoretical predictions [Eq. (D2)].

and grows in the stationary probability density of x_a as ε is increased.

Note that $T_{X_a}(0, c) > T_{U_a}(0, c)$ holds from Eqs. (25) and (26). Thus the mutual inhibition between x_a and x_r makes the time it takes x_a to go from 0 to c longer than that for u_a.

IV. DISCUSSION

We can generalize Eqs. (4) and (5) as

$$\frac{dx_a}{d\tau} = \frac{u_a}{\rho_r(x_r)} - x_a, \tag{27}$$

$$\frac{dx_r}{d\tau} = \frac{u_r}{\rho_a(x_a)} - x_r, \tag{28}$$

where $\rho_r(x_r)$ and $\rho_a(x_a)$ are differentiable functions of x_r and x_a satisfying $\rho_r(0), \rho_a(0) > 0$, $\frac{d\rho_r}{dx_r}(x_r) > 0$ for $x_r \geqslant 0$ and $\frac{d\rho_a}{dx_a}(x_a) > 0$ for $x_a \geqslant 0$. Without loss of generality, we can assume that $\rho_r(0) = \rho_a(0) = 1$. Assuming that Eq. (8) defines a well-defined change of variables $u_a = x_a\rho_r(x_r)$ and $u_r = x_r\rho_a(x_a)$, the stationary probability density of (x_a, x_r) in this case is given by

$$P(x_a, x_r) = Q_a[x_a\rho_r(x_r)]Q_r[x_r\rho_a(x_a)] \times \left(\rho_r(x_r)\rho_a(x_a) - x_a x_r \frac{d\rho_r}{dx_r}(x_r)\frac{d\rho_a}{dx_a}(x_a)\right) \tag{29}$$

from Eq. (11).

The condition that $P_a(x_a)$ has a peak at $x_a = 0$ [Eq. (17)] is

$$\frac{d\ \ln Q_a}{du_a}(0) = \frac{2A_a(0) - \frac{dB_a}{du_a}(0)}{B_a(0)} < \frac{2\frac{d\rho_a}{dx_a}(0)\left\langle U_r \frac{d\rho_r}{dx_r}(U_r)\right\rangle}{\langle \rho_r(U_r)^2\rangle}, \tag{30}$$

which can be derived by a similar calculation as that in Appendix A. Here, $\rho_r(U_r)$ and $\frac{d\rho_r}{dx_r}(U_r)$ are stochastic variables obtained by substituting U_r into x_r in $\rho_r(x_r)$ and $\frac{d\rho_r}{dx_r}(x_r)$, respectively. Equation (30) becomes Eq. (18) when $\rho_r(x_r) = 1 + x_r$ and $\rho_a(x_a) = 1 + x_a$. Similar to the result obtained in Sec. III A, $P_a(x_a)$ can have a peak at $x_a = 0$ even when $\frac{dQ_a}{du_a}(0) > 0$ so long as Eq. (30) holds. Note that the right-hand side of Eq. (30) is positive when U_r has a positive average as in the case of Eq. (18) [for example, when $B_r(u_r)$ is positive and $A_r(u_r)$ is an arbitrary function so long as Eqs. (6) and (7) are well defined] since $\frac{d\rho_a}{dx_a}(0) > 0$ and $\langle U_r \frac{d\rho_r}{dx_r}(U_r)\rangle \geqslant \langle U_r\rangle \frac{d\rho_a}{dx_r}(0) > 0$. Thus the emergence of a peak at $x_a = 0$ is not restricted to the specific form of mutual inhibition as in Eqs. (4) and (5), but is a generic phenomenon.

Apparently similar noise-induced transitions from a unimodal to a bimodal stationary probability density have been reported in various systems [6–8,11,16,17]. Such transitions can be induced by either extrinsic noise [11,16,17] or intrinsic noise [6–9]. In these previous studies, the deterministic part of the model equation typically had a single globally stable equilibrium point. The transition from a unimodal density peaked at the equilibrium point to a bimodal density was caused by inhomogeneous multiplicative noise: if the noise strength is stronger than the rest of the phase space around the equilibrium point, then the orbit of the system's state stays less frequently around the equilibrium point and the relative frequency to visit the rest of the phase space increases. In particular, if the dimension of the phase space is 1 and it is a finite interval, then the stationary probability density can have two peaks around the two end points of the phase space interval [7,8].

The mechanism for the transition presented in this paper seems to be different from that for the noise-induced transition mentioned above. In the main example, we observed that $P_a(x_a)$ can have a peak at $x_a = 0$ even when $P(x_a, x_r)$ does not have one on the line $x_a = 0$. The emergence of this left-side peak in $P_a(x_a)$ is due to the marginalization of $P(x_a, x_r)$ and the mutual inhibition defining the change of variables which deforms $Q_a(u_a)Q_r(u_r)$ to $P(x_a, x_r)$ so that the latter has more mass in the region with small x_a.

The peak at $x_a = 0$ in $P_a(x_a)$ represents an "inactive" state in contrast to the "active state" represented by the peak at $x_a = x_a^*$. Since $P_a(x_a)$ is the marginal density of $P(x_a, x_r)$, this inactive state includes a continuous spectrum of inhibition strength: from no inhibition $x_r = 0$ to the maximum inhibition $x_r = \nu_r$. As we observed in the calculation of the mean first passage time from $x_a = 0$ to $x_a = c$ $(0 < c \leqslant x_a^*)$, the smaller the strength of inhibition at $x_a = 0$, the easier it is to reach $x_a = c$. Thus the transition from the inactive state to the "active" state and vice versa typically occurs by passing through the "gate" region where both x_a and x_r have small values. Construction of such an inactive state could provide a possible basis for diversity in decision making in biological systems [13].

In conclusion, a different type of noise-induced transition from a unimodal to a bimodal stationary probability density occurs in a simple mutual inhibition system with slow fluctuating responses to external signals. The transition is not dependent on the specific form of mutual inhibition used in this paper and should be considered a generic property.

ACKNOWLEDGMENT

This work was supported by JSPS KAKENHI Grant No. JP20K11948.

APPENDIX A: DERIVATION OF EQ. (18)

Assume that $x_a < x_a^*$ holds. Then, $\frac{\nu_r}{x_a+1} < \frac{\nu_a}{x_a} - 1$. Put $f(x_a) = \frac{\nu_r}{x_a+1}$. Thus Eq. (15) becomes

$$P_a(x_a) = \int_0^{f(x_a)} dx_r P(x_a, x_r), \tag{A1}$$

where $P(x_a, x_r)$ is given by Eq. (12). We have

$$\frac{dP_a}{dx_a}(x_a) = P(x_a, f(x_a))\frac{df}{dx_a}(x_a) + \int_0^{f(x_a)} dx_r \frac{\partial P}{\partial x_a}(x_a, x_r). \tag{A2}$$

The goal is to compute $\frac{dP_a}{dx_a}(0)$. Since $\frac{df}{dx_a}(x_a) = \frac{-\nu_r}{(x_a+1)^2}$ and

$$\begin{aligned}\frac{\partial P}{\partial x_a}(x_a, x_r) &= \frac{dQ_a}{du_a}[x_a(x_r+1)](x_r+1)Q_r[x_r(x_a+1)](x_a+x_r+1)\\ &\quad + Q_a[x_a(x_r+1)]\frac{dQ_r}{du_r}[x_r(x_a+1)]x_r(x_a+x_r+1) + Q_a[x_a(x_r+1)]Q_r[x_r(x_a+1)],\end{aligned} \tag{A3}$$

we obtain

$$\begin{aligned}\frac{dP_a}{dx_a}(0) &= P(0, f(0))\frac{df}{dx_a}(0) + \int_0^{f(0)} dx_r \frac{\partial P}{\partial x_a}(0, x_r)\\ &= -Q_a(0)Q_r(\nu_r)\nu_r(\nu_r+1) + \frac{dQ_a}{du_a}(0)\int_0^{\nu_r} dx_r Q_r(x_r)(x_r+1)^2\\ &\quad + Q_a(0)\int_0^{\nu_r} dx_r \frac{dQ_r}{du_r}(x_r)x_r(x_r+1) + Q_a(0)\int_0^{\nu_r} dx_r Q_r(x_r)\\ &= \frac{dQ_a}{du_a}(0)\int_0^{\nu_r} dx_r Q_r(x_r)(x_r+1)^2 - 2Q_a(0)\int_0^{\nu_r} dx_r Q_r(x_r)x_r,\end{aligned} \tag{A4}$$

where we used integration by parts to compute the third term in the second line. It is straightforward to obtain Eq. (18) from Eq. (A4).

APPENDIX B: EXPLICIT EXPRESSIONS FOR $P_a(x_a)$ AND $P_r(x_r)$ IN THE MAIN EXAMPLE

When $A_a(u_a) = \frac{\Delta_a}{2(u_a+\varepsilon)}$, $B_a(u_a) = \Delta_a$, $A_r(u_r) = 0$, and $B_r(u_r) = \Delta_r$ in Eqs. (6) and (7), Eqs. (15) and (16) are

$$P_a(x_a) = \begin{cases} c_a c_r\left(\nu_r(x_a+\varepsilon) + \frac{\nu_r^2(x_a+\varepsilon)}{2(x_a+1)^2} + \frac{\nu_r^2 x_a}{2(x_a+1)} + \frac{\nu_r^3 x_a}{3(x_a+1)^3}\right) & \text{if } x_a < x_a^*,\\ c_a c_r\left(\frac{(x_a+1)(\nu_a-x_a)(x_a+\nu_a+2\varepsilon)}{2x_a} + \frac{(\nu_a-x_a)^2(x_a+2\nu_a+3\varepsilon)}{6x_a^2}\right) & \text{otherwise}\end{cases} \tag{B1}$$

and

$$P_r(x_r) = \begin{cases} c_a c_r\left(\frac{\nu_a^2(2\nu_a+3\varepsilon)}{6(x_r+1)^2} + \frac{1}{c_a}\right) & \text{if } x_r < x_r^*,\\ c_a c_r\left(\frac{(x_r+1)(\nu_r-x_r)^3}{3x_r^3} + \frac{[(x_r+1)^2+\varepsilon](\nu_r-x_r)^2}{2x_r^2} + \frac{\varepsilon(x_r+1)(\nu_r-x_r)}{x_r}\right) & \text{otherwise},\end{cases} \tag{B2}$$

respectively.

APPENDIX C: STOCHASTIC DIFFERENTIAL EQUATION GOVERNING THE DYNAMICS OF (x_a, x_r) IN THE MAIN EXAMPLE

Stochastic differential equations (6) and (7) are transformed to

$$dx_a = \left(A_a(u_a)\frac{\partial x_a}{\partial u_a} + A_r(u_r)\frac{\partial x_a}{\partial u_r} + \frac{1}{2}B_a(u_a)\frac{\partial^2 x_a}{\partial u_a^2} + \frac{1}{2}B_r(u_r)\frac{\partial^2 x_a}{\partial u_r^2}\right)dt + \sqrt{B_a(u_a)}\frac{\partial x_a}{\partial u_a}dW_a + \sqrt{B_r(u_r)}\frac{\partial x_a}{\partial u_r}dW_r, \tag{C1}$$

$$dx_r = \left(A_a(u_a)\frac{\partial x_r}{\partial u_a} + A_r(u_r)\frac{\partial x_r}{\partial u_r} + \frac{1}{2}B_a(u_a)\frac{\partial^2 x_r}{\partial u_a^2} + \frac{1}{2}B_r(u_r)\frac{\partial^2 x_r}{\partial u_r^2}\right)dt + \sqrt{B_a(u_a)}\frac{\partial x_r}{\partial u_a}dW_a + \sqrt{B_r(u_r)}\frac{\partial x_r}{\partial u_r}dW_r \tag{C2}$$

by applying Ito's formula [14] under the change of variables in Eqs. (9) and (10). We have

$$\frac{\partial x_a}{\partial u_a} = \frac{x_a+1}{x_a+x_r+1}, \quad \frac{\partial x_a}{\partial u_r} = \frac{-x_a}{x_a+x_r+1}, \quad \frac{\partial x_r}{\partial u_a} = \frac{-x_r}{x_a+x_r+1}, \quad \frac{\partial x_r}{\partial u_r} = \frac{x_r+1}{x_a+x_r+1}$$

and

$$\frac{\partial^2 x_a}{\partial u_a^2} = \frac{\partial^2 x_r}{\partial u_a^2} = \frac{2x_r(x_a+1)}{(x_a+x_r+1)^3}, \quad \frac{\partial^2 x_a}{\partial u_r^2} = \frac{\partial^2 x_r}{\partial u_r^2} = \frac{2x_a(x_r+1)}{(x_a+x_r+1)^3}.$$

Substituting these and $A_a(u_a) = \frac{\Delta_a}{2(u_a+\varepsilon)}$, $B_a(u_a) = \Delta_a$, $A_r(u_r) = 0$, and $B_r(u_r) = \Delta_r$ into Eqs. (C1) and (C2), we obtain

$$dx_a = \left(\frac{\Delta_a(x_a+1)}{2[x_a(x_r+1)+\varepsilon](x_a+x_r+1)} + \frac{\Delta_a x_r(x_a+1) + \Delta_r x_a(x_r+1)}{(x_a+x_r+1)^3}\right)dt + \sqrt{\Delta_a}\frac{x_a+1}{x_a+x_r+1}dW_a - \sqrt{\Delta_r}\frac{x_a}{x_a+x_r+1}dW_r, \tag{C3}$$

$$dx_r = \left(-\frac{\Delta_a x_r}{2[x_a(x_r+1)+\varepsilon](x_a+x_r+1)} + \frac{\Delta_a x_r(x_a+1) + \Delta_r x_a(x_r+1)}{(x_a+x_r+1)^3}\right)dt - \sqrt{\Delta_a}\frac{x_r}{x_a+x_r+1}dW_a + \sqrt{\Delta_r}\frac{x_r+1}{x_a+x_r+1}dW_r. \tag{C4}$$

Note that Eq. (21) is a stationary solution of Eqs. (C3) and (C4). In particular, it is a potential solution since $Q_a(u_a)Q_r(u_r)$ is. We observe that when ε increases, the drift term of Eq. (C3) decreases and that of Eq. (C4) increases. On the other hand, none of the diffusion terms contain ε. Thus we can expect that the probability density of (x_a, x_r) becomes more biased toward the upper-left corner as ε becomes larger.

APPENDIX D: EXPLICIT EXPRESSION FOR $T_{X_a}(0, c)$ IN THE MAIN EXAMPLE

We take $A_a(u_a) = \frac{\Delta_a}{2(u_a+\varepsilon)}$, $B_a(u_a) = \Delta_a$, $A_r(u_r) = 0$, and $B_r(u_r) = \Delta_r$ in Eqs. (6) and (7). In this case, we have $\psi(u) = \frac{u}{\varepsilon} + 1$. Thus we obtain

$$T_{U_a}(u_a) = \frac{1}{\Delta_a}\left[\frac{u_a^2}{2} + \varepsilon u_a - \varepsilon^2 \ln\left(\frac{u_a}{\varepsilon} + 1\right)\right] \tag{D1}$$

from Eq. (26). Substituting Eqs. (20) and (D1) into Eq. (25) and solving the integral gives

$$T_{X_a}(0, c) = \frac{c+1}{\Delta_a \nu_r c}\left[I\left(\frac{\nu_r c}{c+1} + c\right) - I(c)\right], \tag{D2}$$

where

$$I(c) = \tfrac{1}{6}c^3 + \tfrac{1}{2}\varepsilon c^2 - \varepsilon^2(c+\varepsilon)[\ln(c+\varepsilon) - 1] + (\varepsilon^2 \ln \varepsilon)c. \tag{D3}$$

[1] K. Matsumoto and I. Tsuda, J. Stat. Phys. **31**, 87 (1983).
[2] L. Molgedey, J. Schuchhardt, and H. G. Schuster, Phys. Rev. Lett. **69**, 3717 (1992).
[3] J. N. Teramae and D. Tanaka, Phys. Rev. Lett. **93**, 204103 (2004).
[4] A. J. McKane and T. J. Newman, Phys. Rev. Lett. **94**, 218102 (2005).
[5] Q. Li and X. Lang, Biophys. J. **94**, 1983 (2008).
[6] Y. Togashi and K. Kaneko, Phys. Rev. Lett. **86**, 2459 (2001).
[7] J. Ohkubo, N. Shnerb, and D. A. Kessler, J. Phys. Soc. Jpn. **77**, 044002 (2008).
[8] T. Biancalani, L. Dyson, and A. J. McKane, Phys. Rev. Lett. **112**, 038101 (2014).
[9] M. Jozsa, T. I. Donchev, R. Sepulchre, and T. O'Leary, Proc. Natl. Acad. Sci. USA **119**, e2116054119 (2022).
[10] C. V. Rao, D. M. Wolf, and A. P. Arkin, Nature (London) **420**, 231 (2002).
[11] T. J. Kobayashi, Phys. Rev. Lett. **106**, 228101 (2011).
[12] U. Alon, *Introduction to Systems Biology, Second Edition* (Chapman and Hall/CRC, Boca Raton, FL, 2020).
[13] T. Shirakawa, Y.-P. Gunji, H. Sato, and H. Tsubakino, Int. J. Unconv. Comput. **15**, 275 (2020).
[14] C. W. Gardiner, *Stochastic Methods, Fourth Edition* (Springer-Verlag, Berlin, Heidelberg, 2009).
[15] See Supplemental Material at http://link.aps.org/supplemental/10.1103/PhysRevE.108.024108 for the analysis of the model including z and the discussion on the origin of "weak bimodality."
[16] W. Horsthemke and R. Lefever, *Noise-Induced Transitions* (Springer-Verlag, Berlin, 1984).
[17] T. Haruna, Artif. Life Robot. **24**, 297 (2019).